JCTC Journal of Chemical Theory and Computation

Article

pubs.acs.org/JCTC

Global Flux Surface Hopping Approach for Mixed Quantum-Classical Dynamics

Linjun Wang,*[,†] Dhara Trivedi,[‡] and Oleg V. Prezhdo*[,†,‡]

[†]Department of Chemistry, University of Rochester, Rochester, New York 14627, United States

[‡]Department of Physics & Astronomy, University of Rochester, Rochester, New York 14627, United States

ABSTRACT: A novel global flux surface hopping (GFSH) approach is proposed. In this method, the surface hopping probabilities rely on the gross population flow between states, rather than the state-to-state flux as in the standard fewest switches surface hopping (FSSH). GFSH captures the superexchange mechanism of population transfer, while FSSH lacks this capability. In other aspects, including minimization of the number of hops, internal consistency, velocity rescaling, and detailed balance, the GFSH algorithm is similar to FSSH. The advantages of GFSH are demonstrated with a model 3-level system and an Auger process in a semiconductor quantum dot. Current studies indicate that GFSH can replace FSSH, but further tests are needed.

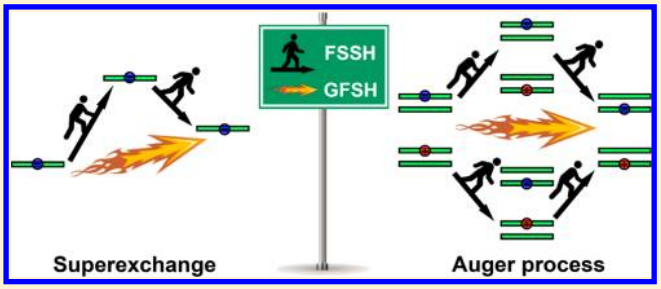

1. INTRODUCTION

The majority of physical, chemical, and biological systems of current scientific interest contain a large number of degrees of freedom. On one hand, the observed phenomena cannot be described in a fully quantum manner due to the high theoretical complexity and computational cost. On the other hand, purely classical approaches are unlikely to achieve accurate descriptions for a variety of dynamical processes involving significant quantum effects, for example, proton transfer,[1,2] exciton dynamics,[3−5] electron transfer,[6−8] charge transport,[9−11] and high-frequency vibrational energy relaxation.[12,13] At the present stage, mixed quantum-classical dynamics (MQCD) provide the most popular and reliable solution.[14−16] Only a small subset of highly quantum particles, that is, protons, excitons, electrons, holes, and phonons, are dealt with quantum mechanically, while the remaining parts of the system are treated classically.

The feedback between the quantum and concomitant classical subsystems constitutes a major issue in MQCD. Namely, the quantum wave function should evolve correctly under the influence of a classical trajectory. In turn, the classical motion should depend properly on the quantum propagation.[17,18] The primary and simplest attempt is the Ehrenfest approach,[19,20] in which the classical dynamics experience a single averaged potential energy surface (PES) generated by the quantum variables. Such mean-field (MF) behavior is most apparent in situations where the quantum and classical subsystems are weakly coupled.[9] However, when classical trajectories rely strongly on particular realizations of the quantum evolution, the MF approximation becomes inadequate. This problem can be corrected by means of the surface hopping (SH) idea,[21−24] where one introduces stochastic quantum hops between preferred quantum states. In recent years, a lot of effort has been invested to combine SH with ab initio calculations to simulate time-domain dynamical properties.[25−31]

Because of its appealing simplicity, ease of implementation, and computational efficiency, Tully's fewest switches surface hopping (FSSH) algorithm[21] (also called molecular dynamics with quantum transitions or MDQT) has understandably retained its popularity. Tully's seminal work,[21] published in 1990, has been cited over a thousand times so far. Within the FSSH formalism, the classical particles evolve on one PES through Newtonian equations, the quantum parts are propagated according to the time-dependent Schrödinger equation, and nonadiabatic transitions between PESs occur stochastically with probabilities determined by quantum-mechanical rules. The FSSH probabilities are designed to minimize the number of state switches.[21]

The FSSH algorithm involves two key characteristics—internal consistency and energy conservation. The internal consistency ensures that the fraction of trajectories on each PES is equivalent to the corresponding average quantum probability determined by coherent propagation of the quantum amplitudes. The internal consistency may be violated when one encounters trivial crossings,[10,32−36] where the energy gaps between PESs are negligible and the finite time step cannot ensure an accurate evaluation of surface hopping probabilities. Recently, we have proposed a self-consistent FSSH (SC-FSSH) approach,[36] where a self-consistency check is implemented at each time step to correct the surface hopping probabilities. Extremely high accuracy is achieved along with a significantly reduced computational cost. Even more serious, a violation of internal consistency arises due to the existence of classically

Received: May 1, 2014
Published: June 12, 2014

   dx.doi.org/10.1021/ct5003835 | J. Chem. Theory Comput. 2014, 10, 3598−3605

forbidden transitions in standard FSSH.[37] Such frustrated hops violating the energy conservation are excluded and thus break the self-consistency argument to justify the FSSH algorithm. At the same time, frustrated hops provide a mechanism to achieve a detailed balance of transitions upward and downward in energy, leading to thermodynamic equilibrium.[17] Solutions of the Schrödinger equation driven by a classical trajectory, the so-called classical path approximation (CPA),[31] as well as the Ehrenfest approach, does not achieve the equilibrium, and therefore cannot describe, for instance, electron-vibrational energy relaxation ubiquitous in applications.[29−31]

Several approaches have been proposed to eliminate classically forbidden transitions. For instance, one can change the direction of the nuclear momentum as though the trajectory hits a barrier as it tries to hop.[1] In this aspect, the trajectory continues without changing the active electronic state. However, it was found that such prescription does not evidently improve the surface hopping performance.[37] There also exists the modified MDQT* method,[38,39] which invokes modified velocities in the integration of the quantum amplitudes. In comparison with the standard FSSH, the MDQT* method leads to remarkable internal consistency. However, as emphasized by the authors, MDQT* is not based on rigorous theoretical grounds.[38,39] Jasper and coauthors have proposed a series of fewest-switches with time uncertainty (FSTU) methods,[40,41] which incorporate quantum uncertainty into the surface hopping time. FSTU can remove frustrated hops because it allows a trajectory experiencing a classically forbidden transition, to hop nonlocally to a geometry along the trajectory, where the hop becomes classically allowed. Although FSTU is found to achieve better accuracy than FSSH, the classical trajectories become discontinuous. Granucci and Persico argued that an accurate transition probability cannot be obtained when the trajectories are run independently.[42] The introduction of interdependence among trajectories breaks the computational simplicity of SH and is quite time-consuming for practical calculations. It should be emphasized that one cannot and should not fully avoid classically forbidden transitions, because they are necessary to realize the detailed balance in surface hopping simulations.[17,18]

Superexchange is a class of dynamical processes, where two electronic states are coupled indirectly through an intermediate state with a higher energy (see Figure 1A). In these cases, electron transfer proceeds through the intermediate virtual state, which is hardly populated. A typical example of superexchange is singlet fission, where a singlet excitation converts to a triplet pair state in virtue of charge transfer states.[43−46] Singlet fission is a spin-allowed process, which can potentially double the number of electron−hole pairs and thus largely increase the efficiency of organic photovoltaics.[47] As shown in Figure 1A, step I of superexchange experiences a large energy barrier, and thus hops to the state 2 can be classically forbidden in the standard FSSH. Auger phenomena constitute a broad class of processes,[48−50] represented by the electron−hole energy exchange (Figure 1B). This mechanism may dominate the fast electron relaxation in colloidal semiconductor quantum dots (QDs).[49,50] The Auger process is a two-particle reaction, which also proceeds with intermediate states. Similar to the superexchange of Figure 1A, steps I and IV in Figure 1B can be classically inaccessible, and thus cannot be described properly within FSSH.

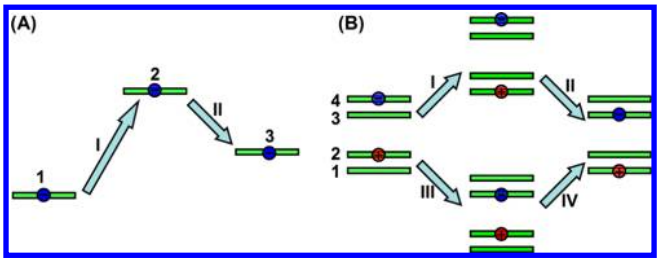

Figure 1. Schematic representation of (A) superexchange and (B) Auger processes. Electron and hole are expressed with ⊖ and ⊕, respectively. States are labeled by Arabic numbers, and pathways between states are indicated with arrows and Roman numbers.

In this study, we propose an alternative strategy for surface hopping. Conservation of the total population of all states during quantum evolution constitutes the starting point of the new method. This naturally implies population flow, and thus surface hopping probability, from states with reduced population to states with increased population. Our approach is virtually identical to FSSH, except that we set the surface hopping probabilities according to the global flux of population change instead of the state-to-state flux derived by Tully.[21] Hence, we call the technique global flux surface hopping (GFSH). Minimization of the total number of hops was a key motivation behind Tully's FSSH derivation. The new method also uses a flux of populations rather than their absolute values, and therefore, it also minimizes the number of hops, similarly to FSSH. The advantages of GFSH are illustrated with a superexchange model and an Auger process in a semiconductor QD.

2. METHODOLOGY

2.1. Hamiltonian and Equations of Motion. Consider a system consisting of both quantum and classical particles, whose coordinates are expressed by **r** and **R**, respectively. The total Hamiltonian can be written as

$$H = T_R + H_0(\mathbf{r}, \mathbf{R}) \tag{1}$$

where T_R is the kinetic energy operator for classical motions, and $H_0(\mathbf{r},\mathbf{R})$ is the quantum part of the Hamiltonian as a function of classical positions. If we implement an orthonormal set of electronic basis functions, $\{\phi_i(\mathbf{r};\mathbf{R})\}$, that depends parametrically on **R**, we can define matrix elements of $H_0(\mathbf{r},\mathbf{R})$ as

$$V_{ij}(\mathbf{R}) = \langle \phi_i(\mathbf{r};\mathbf{R}) | H_0(\mathbf{r},\mathbf{R}) | \phi_j(\mathbf{r};\mathbf{R}) \rangle \tag{2}$$

We expand the wave function of quantum particles in terms of the basis functions as

$$\psi(\mathbf{r},\mathbf{R}) = \sum_i c_i |\phi_i(\mathbf{r};\mathbf{R})\rangle \tag{3}$$

Substituting eq 3 into the time dependent Schrödinger equation,

$$i\hbar \frac{d\psi(\mathbf{r},\mathbf{R})}{dt} = H_0(\mathbf{r},\mathbf{R})\psi(\mathbf{r},\mathbf{R}) \tag{4}$$

results in

$$i\hbar \dot{c}_i = \sum_j c_j (V_{ij} - i\hbar \dot{\mathbf{R}} \cdot \mathbf{d}_{ij}) \tag{5}$$

dx.doi.org/10.1021/ct5003835 | J. Chem. Theory Comput. 2014, 10, 3598−3605

where $d_{ij}(\mathbf{R}) \equiv \langle \phi_i(\mathbf{r};\mathbf{R})|\nabla_R \phi_j(\mathbf{r};\mathbf{R})\rangle$ are nonadiabatic coupling vectors. Then, the time dependence of the density matrix elements, $a_{ii} = c_i c_j^*$, can be deduced as

$$\dot{a}_{ij} = \sum_{j\neq i} b_{ij} \tag{6}$$

where

$$b_{ij} = 2\hbar^{-1}\mathrm{Im}(a_{ij}^* V_{ij}) - 2\mathrm{Re}(a_{ij}^* \dot{\mathbf{R}}\cdot\mathbf{d}_{ij}) \tag{7}$$

2.2. FSSH. In standard FSSH, according to practical requirements, we initially set the positions and momenta of classical particles, as well as the wave function and active state of quantum observables. The classical degrees of freedom are evolved on the active PES i according to the corresponding Newtonian equation,

$$\dot{\mathbf{P}}_k = -\partial V_{ii}/\partial \mathbf{R}_k \tag{8}$$

where $\mathbf{R}_k$ and $\mathbf{P}_k$ are the k-th component of the collective coordinates and momenta of the classical particles. The wave function evolution is carried out according to eq 5. At every time step dt, the switching probabilities from the current active state i to all other states j are computed from the density matrix elements based on eq 7 as

$$g_{ij} = \max\left\{\frac{-\mathrm{d}t\cdot b_{ij}}{a_{ii}}, 0\right\} \tag{9}$$

In order to determine whether there is a surface hop, a uniform random number $\xi \in (0,1)$ is generated and compared with the surface hopping probabilities given by eq 9. When $\sum_{j=1}^{j=k-1} g_{ij} < \xi < \sum_{j=1}^{j=k} g_{ij}$, the active PES is expected to switch from i to k. There, one needs to adjust velocities to conserve the total energy, and this velocity adjustment is normally performed in the direction of the nonadiabatic coupling vector.[21] It is possible that the component of the velocity to be adjusted is less than the velocity reduction required to make the surface hop, then the state switch cannot be invoked, resulting in a classically forbidden transition. The above procedure is repeated until the trajectory is declared finished by an appropriate criterion. A certain number of realizations are needed to achieve converged results.

It is important to note that the FSSH probability between states i and j, eq 9, depends explicitly on the coupling between these states, either diabatic, V_{ij}, or nonadiabatic $\mathbf{d}_{ij}$, eq 7. Therefore, if the states are not coupled directly, transitions between them are not possible.

2.3. GFSH. Most of the steps in GFSH are identical to FSSH. The major difference lies in the setup of the surface hopping probabilities. Instead of using eq 9 for a time step $[t,t+\mathrm{d}t]$, we examine the population change of all quantum states,

$$\Delta a_{ii} = a_{ii}(t+\mathrm{d}t) - a_{ii}(t) \tag{10}$$

and classify the states into two subgroups: one with reduced population (group A), and the other with increased population (group B). Since the total population of the system is always unity, the gross population decrease in group A equals to the total population increase in group B. Therefore, it is natural to expect surface hops from group A to group B. If the current active state belongs to group A, the surface hopping probability from i to any state j in B should be proportional to the population increase of state j. Besides, this increased population could come from all possible states in group A, where the contribution from state i relies on the ratio of its population decrease with respect to the total population reduction in group A. Hence, the surface hopping probabilities can be expressed as

$$g_{ij} = \frac{\Delta a_{jj}}{a_{ii}} \frac{\Delta a_{ii}}{\sum_{k\in A}\Delta a_{kk}} \quad (\text{if } i\in A \text{ and } j\in B) \tag{11}$$

All other types of state switches (i.e., between states within the same group or from group B to A) are not expected to happen. Once a surface hop is decided in GFSH, energy conservation is strictly enforced the same way as in FSSH. The nuclear velocity in the direction of the nonadiabatic coupling is rescaled to reflect the change in the electronic energy. In superexchange cases, the nonadiabatic coupling between the initial and final states is zero, and the velocity rescaling direction is not defined. Then, one should consider the second (or higher) order nature or superexchange and define projections of the corresponding sequence of nonadiabatic couplings. For instance, if states i and j are coupled via state k, one projects $\mathbf{d}_{ik}$ on $\mathbf{d}_{kj}$ to define the scaling direction. If there is a set of intermediate states k, one can define the scaling direction by adding the projections of $\mathbf{d}_{ik}$ on $\mathbf{d}_{kj}$ for all k.

It is important to note that GFSH is identical to FSSH for systems involving only two quantum states. This is true since, in the two state limit, eq 11 reduces to eq 9, per eqs 6, 7, and 10. Thus, GFSH fully reproduces the FSSH results for Tully's two-level models.[21] Due to the clear physical picture and simple formulation of GFSH, as well as the general similarity with FSSH, the existing codes implementing FSSH can be easily modified to carry out GFSH simulations.

2.4. Internal Consistency. Internal consistency is key for the rationality of SH theories. It ensures that the state occupations resulting from SH correspond to the standard quantum mechanical occupations. In order to prove the internal consistency, we first assume that at time t the fraction of trajectories on each PES i (i.e., p_i) is already equivalent to the corresponding quantum probability (i.e., a_{ii}). This can be achieved by the proper choice of initial conditions at $t = 0$. Then, we examine whether the fraction of trajectories after a time step dt still agrees with the quantum probability. If the answer is true, then internal consistency holds for the whole dynamics along one trajectory. Averaging over all trajectories, the fraction of trajectories on each PES equals to the corresponding average quantum probability. In the following, we will show that both standard FSSH and the currently proposed GFSH satisfy the internal consistency.

We start with FSSH. According to eq 7, we have $b_{ji} = -b_{ij}$ and $b_{ii} = 0$. When $i \neq j$, either g_{ij} or g_{ji} is positive and the other one is zero. For any state i, we can classify all other states into two subgroups: one with $g_{ij} > 0$ (group A′), and the other one with $g_{ij} = 0$ (group B′). In group A′, surface hopping happens from i to other states, and the total fraction of trajectories to hop out from state i is $\sum_{j\in A'} g_{ij} a_{ii} = -\sum_{j\in A'} \mathrm{d}t\, b_{ij}$. It is the opposite in group B′, where state switches from other states to i, and the total fraction of trajectories hopping into state i is $\sum_{j\in B'} g_{ji} a_{jj} = \sum_{j\in B'} \mathrm{d}t\, b_{ij}$. As a result, the change in probability to stay on surface i becomes $\sum_{j\in B'} \mathrm{d}t\, b_{ij} - (-\sum_{j\in A'} \mathrm{d}t\, b_{ij}) = \sum_j \mathrm{d}t\, b_{ij}$. According to eq 6, this change in the fraction of trajectories is equal to the population change based on the Schrödinger eq 4. This phenomenon holds for all quantum sates, and thus, the internal consistency is always kept.

In GFSH, we can also classify all states into two subgroups, as discussed previously. There exists only one channel to

dx.doi.org/10.1021/ct5003835 | J. Chem. Theory Comput. 2014, 10, 3598−3605

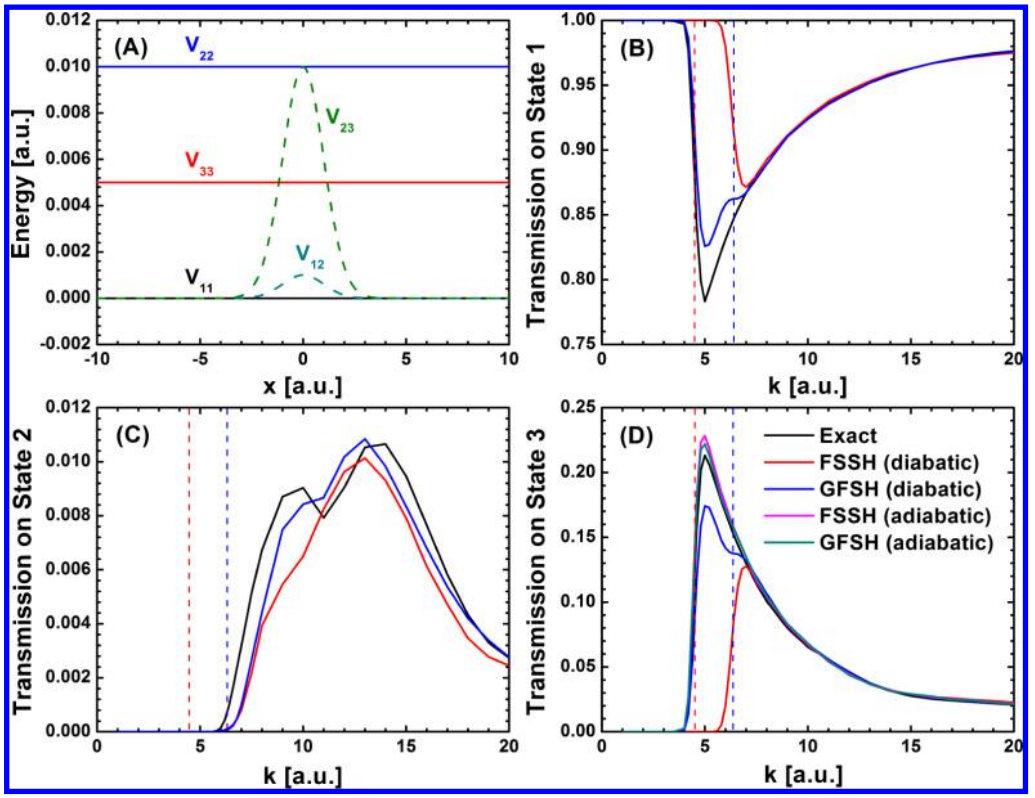

Figure 2. (A) Diabatic potential energy surfaces and interstate couplings of the adopted superexchange model, and transmission on (B) first, (C) second, and (D) third states obtained from exact quantum dynamics, FSSH, and GFSH in diabatic and adiabatic representations. The vertical red (blue) dashed lines express the critical momenta which give the kinetic energies equaling to the energy gap between the third (second) and the first states.

change the fraction of trajectories in state i from group A, via surface hops to any state in group B. The total fraction of trajectories to hop out is $\Sigma_{j\in B} g_{ij}\, a_{ii} = \Sigma_{j\in B}\Delta a_{jj}\, \Delta a_{ii}/(\Sigma_{k\in A}\Delta a_{kk})$. The total population reduction is the same as the total population increase, that is, $\Sigma_{j\in B}\Delta a_{jj} = -\Sigma_{k\in A}\Delta a_{kk}$; thus, the total fraction of trajectories to hop out of state i becomes $\Sigma_{j\in B} g_{ij} a_{ii} = -\Delta a_{ii}$, which is exactly the inverse number of population change based on the Schrödinger equation. Similarly, there is also only one channel to change the fraction of trajectories in state j from group B, via surface hops from all possible states in group A to state j. The total fraction of trajectories to hop into state j is $\Sigma_{i\in A} g_{ij} a_{ii} = \Sigma_{i\in A}\Delta a_{ii}\ \Delta a_{jj}/(\Sigma_{k\in A}\Delta a_{kk}) = \Delta a_{jj}$. This corresponds to the population change of state j according to the Schrödinger equation. Therefore, GFSH also satisfies the internal consistency.

2.5. Wave Packet Propagation. In the numerical calculations below, we will compare the performance of FSSH and GFSH for a representative superexchange model. In order to reveal the accuracy of SH simulations prominently, we need the exact quantum solutions. To this end, we employ explicitly the wave packet propagation procedure reported by Kosloff et al.[51] We use a three-state model, with basis functions |1>, |2>, and |3>, coupled to a one-dimensional continuous nuclear degree of freedom, x, and express the wave function for the whole system as $\psi = c_1(x)|1> + c_2(x)|2> + c_3(x)|3>$. The corresponding Schrödinger equation reads

$$i\hbar\begin{pmatrix}\dot{c}_1\\ \dot{c}_2\\ \dot{c}_3\end{pmatrix} = -\frac{\hbar^2}{2m}\begin{pmatrix}\partial^2 c_1/\partial x^2\\ \partial^2 c_2/\partial x^2\\ \partial^2 c_3/\partial x^2\end{pmatrix} + \begin{pmatrix}V_{11} & V_{12} & V_{13}\\ V_{21} & V_{22} & V_{23}\\ V_{31} & V_{32} & V_{33}\end{pmatrix}\begin{pmatrix}c_1\\ c_2\\ c_3\end{pmatrix} \tag{12}$$

where V_{ij} is the matrix elements of the quantum Hamiltonian in eq 2. The terms $\partial^2 c_i/\partial x^2$ can be obtained by means of the fast Fourier transform (FFT) technique in a discrete representation.[52] Suppose x falls within a range of L, which is divided into N parts, $\partial^2 c_i/\partial x^2$ can be expressed as $\partial^2 c_i(x)/\partial x^2 = N^2/L^2\ \partial^2 c_i(n)/\partial n^2$. Since the discrete Fourier transformation (FT) for $c_i(n)$ can be expressed as $c_i(k) = \Sigma_{n=0}^{N-1} c_i(n) e^{-i2\pi kn/N}$, and the corresponding inverse Fourier transformation (IFT) reads $c_i(n) = (1/N)\ \Sigma_{k=0}^{N-1} c_i(k) e^{i2\pi kn/N}$, we can easily derive that

$$\partial^2 c_i/\partial x^2 = \frac{4\pi^2}{L^2}\frac{1}{N}\sum_{k=0}^{N-1}[-k^2 c_i(k)] e^{i2\pi kn/N} \tag{13}$$

Thus, we can perform FT for $c_i(n)$ to get $c_i(k)$, multiply it by $-k^2$ for the corresponding components, and carry out IFT to get $\partial^2 c_i/\partial x^2$. Then eq 12 can be solved iteratively with the standard fourth-order Runge−Kutta (RK4) algorithm.[53]

3. RESULTS AND DISCUSSION

3.1. Superexchange Model. Our model for superexchange is a three-state system defined by the following state energies and interstate couplings in the diabatic representation: $V_{11}(x) = 0$, $V_{22}(x) = 0.01$, $V_{33}(x) = 0.005$, $V_{12}(x) = V_{21}(x) = 0.001\ e^{-x^2/2}$, $V_{23}(x) = V_{32}(x) = 0.01\ e^{-x^2/2}$, and $V_{13}(x) = V_{31}(x) = 0$. All these parameters are given in

dx.doi.org/10.1021/ct5003835 | J. Chem. Theory Comput. 2014, 10, 3598−3605

atomic units. The state energies are constant, and the interstate couplings are localized within the interaction region $-2.5 < x < 2.5$ (see Figure 2A). The model represents the superexchange mechanism of transitions from state 1 to state 3 via state 2: states 1 and 3 are not coupled directly, while both 1 and 3 are coupled to state 2.

Similar with Tully's models,[21] the mass is chosen to be 2000 a.u., which is close to the mass of a hydrogen atom, thus significant quantum effects are expected. The wave packet was initially prepared in the first diabatic state, and chosen to be Gaussian, that is, $c_1(x) = \exp(ikx)\exp[-(x - x_0)^2/\sigma^2]$, and $c_2(x) = c_3(x) = 0$. Here, the initial mean coordinate, x_0, is negative, lying outside of the interaction region. The momentum, k, is a positive number. The width of the packet, σ, is chosen to be 20 times the inverse of the momentum k. Thus, the initial wave packet has an energy spread of about ±10% of its initial energy, allowing some damping of quantum interference between the three states.[21] In the quantum dynamics, the equations of motion in eq 12 were integrated with the standard RK4 method[53] coupled with the FFT technique[52] until the wave packet completely left the interaction region.

In Figure 2B–D, we compare the transmissions on different states obtained from the quantum mechanical standard, FSSH, and GFSH. FSSH and GFSH are performed in the diabatic representation, which represents the superexchange mechanism of transitions between states 1 and 3 by coupling via state 2. While FSSH and GFSH can be performed in the adiabatic representation as well,[10,11,36,54] the adiabatic model does not represent superexchange, because nonadiabatic coupling exists between all pairs of states. In the adiabatic representation of the present model, the GFSH results are very close to FSSH, even showing a slight improvement (Figure 3D). Note that there is no probability for reflections on any state due to the flat diabatic PES as well as the positive momenta implemented.

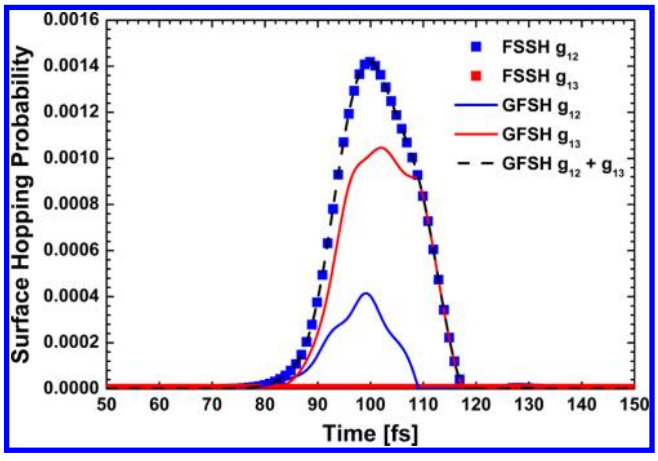

Figure 3. Time-dependent surface hopping probabilities calculated by FSSH and GFSH. The trajectory runs along the first diabatic state. The initial momentum k is set to be 5 a.u., falling inside the superexchange regime.

The results can be analyzed by dividing all investigated momenta into three regimes. In the first regime the kinetic energy, $k^2/2m$, is less than the energy difference between the third and first diabatic states, $V_{33}-V_{11}$. Both FSSH and GFSH agree with the quantum standard. There, the particle remains in the first state after crossing the interaction region. In the second regime the kinetic energy is larger than $V_{33}-V_{11}$ but smaller than $V_{22}-V_{11}$. The exact solution shows significant transmission on the third state, illustrating the superexchange mechanism. In standard FSSH, such a transmission is effectively blocked because (1) the direct transition probability from the first state to the third state is exactly zero as shown in Figure 3 and (2) the indirect pathway relies on surface hopping to the second state, which is classically forbidden. In contrast, GFSH has a large surface hopping probability to the third state (see Figure 3) and can reproduce most of the transmission (see Figure 2D). Note that the total surface hopping probabilities out of the first state are the same in FSSH and GFSH (see Figure 3). GFSH equations are a step closer than FSSH to the solution the time-dependent Schrödinger equation: GFSH probabilities do not explicitly depend on b_{ij} from eq 7 and operate directly with a_{ii} from eq 6. As a result, the superexchange mechanism of transitions between states 1 and 3 included in the Schrödinger equation is also present in GFSH.

In the third regime, where the kinetic energy is higher than $V_{22}-V_{11}$, all adopted methods give similar results again. There, no classically forbidden transitions exist, and the performances of FSSH and GFSH are similar. Note that GFSH gives better descriptions than FSSH for the transmission on the intermediate state shown in Figure 2C, even though the magnitude of the signal is quite small. Thereby, we can conclude that GFSH generally behaves similarly to FSSH when FSSH is appropriate. At the same time, GFSH agrees much better with the exact solutions when encountering classically forbidden transitions. That is to say, the current tests indicate that GFSH can replace FSSH, but further tests are needed.

3.2. Auger Process in a Quantum Dot. As a demonstration of the GFSH method for a realistic application, we choose a small QD (see Figure 4A) and investigate the electron relaxation dynamics. Due to spatial confinement, the electron levels in QDs are well separated in energy, providing a good opportunity for collection of hot carriers (see Figure 4B).[55] These separated electronic energies lead to a large mismatch between the electronic and vibrational energy quanta, significantly impeding the electron–phonon relaxation process, known as the phonon bottleneck effect.[56,57] Many time-resolved experiments, however, have shown much faster, bulk-like relaxation.[50] It is rationalized by the Auger-type energy exchange between the electron and hole, followed by a rapid hole-phonon relaxation in the dense manifold of valence band (VB) states (see Figure 4B). Here, we study the Auger electron–hole energy exchange.

Using the Vienna Ab initio Simulation Package (VASP),[58−60] the QD is fully optimized, equilibrated at 300 K, and evolved microcanonically in the ground electronic state to provide input for FSSH and GFSH. The Kohn–Sham molecular orbitals and the corresponding nonadiabatic couplings are calculated at each time step. This time dependent information is stored, and used to perform the nonadiabatic molecular dynamics (NA-MD) within the recently developed PYthon eXtension for Ab Initio Dynamics (PYXAID) program.[3,4] There, the CPA is implemented to achieve considerable computational savings. To further reduce the computational cost while maintaining the numerical accuracy, we include only the two lowest unoccupied states (the $1P_e$ and $1S_e$ states shown in Figures 4B), and 13 highest occupied states for NA-MD. Tests have shown that including more orbitals in the calculations makes little difference for the results. Initially, the electron is in the $1P_e$ state, and the hole is in the VB maximum (VBM). We use the

dx.doi.org/10.1021/ct5003835 | J. Chem. Theory Comput. 2014, 10, 3598–3605

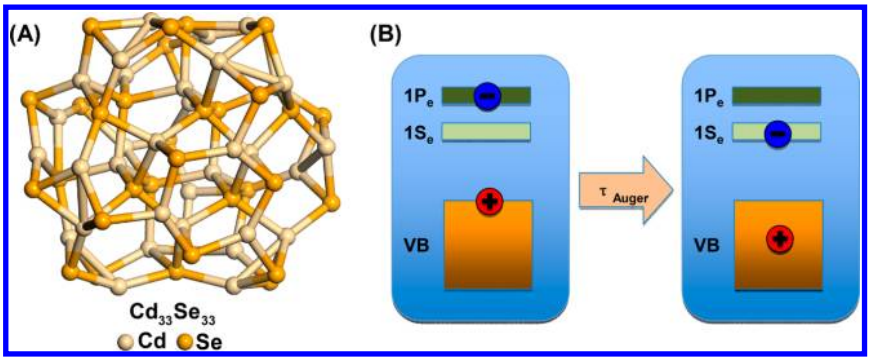

Figure 4. (A) $Cd_{33}Se_{33}$ QD investigated in this study. (B) Schematic representation of the Auger process. The key molecular orbitals include the lowest unoccupied state ($1S_e$), the second lowest unoccupied state ($1P_e$), and the occupied valence band (VB).

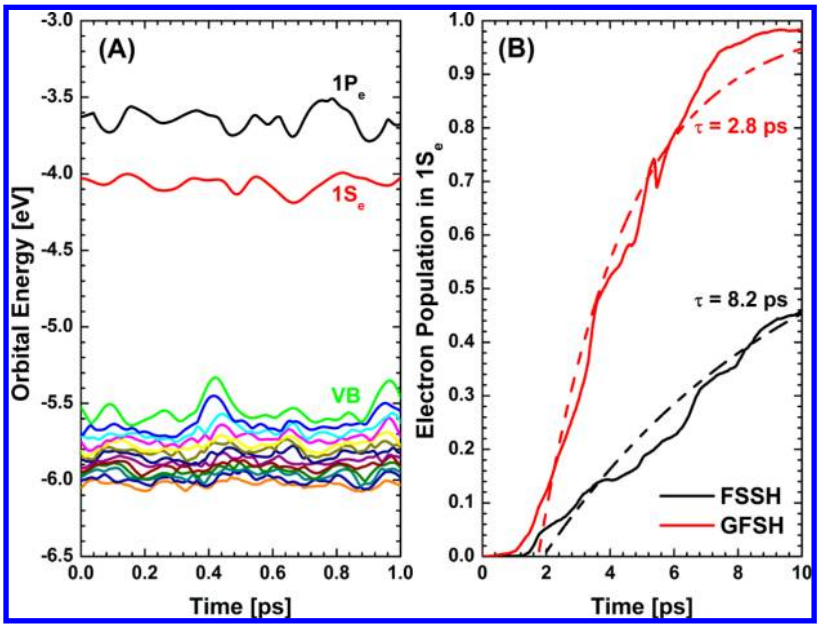

Figure 5. Time evolution of (A) the orbital energies for part of the trajectory and (B) electron population in the $1S_e$ state using FSSH and GFSH.

orbital energies to define the excitations, and employ the CPA for both FSSH and GSFH, as described in refs 3 and 61. We monitor the decay of the electron from the $1P_e$ state to the lowest energy $1S_e$ state, as studied by the pump−probe transient absorption spectroscopy in experiment.[50]

The evolution of the orbital energies for a part of the trajectory is shown in Figure 5A. The obtained mean energy gap between the $1P_e$ and $1S_e$ states is about 0.4 meV, which agrees reasonably well with the experimental observations of 0.1−0.3 eV for CdSe QDs.[50] The larger value arises because the adopted QD is smaller than the experimental QDs. The occupied states are much denser than the unoccupied states. These closely lying occupied states result in fast hole−phonon relaxation dynamics, promoting the overall relaxation when the Auger electron−hole energy exchange channel is open.

In a previous study,[57] it was found that the direct electron transition from $1P_e$ into $1S_e$ is artificially fast due to the lack of decoherence, arising from the quantum mechanical features of the nuclei. In order to eliminate the artificially fast direct electron transition, we remove the corresponding states from the simulation basis. In particular, we restrict the electron−hole basis to the states that reside within ±0.5 eV of the initial excitation, and exclude states in the range between $E_{1S_e}-E_{VBM}$ and $E_{1P_e}-E_{VBM}-0.1$ eV. This ensures that electron relaxation is always accompanied by hole excitation, representing the Auger process.

Figure 5B represents the simulated time evolution of electron population on the $1S_e$ state by both FSSH and GFSH methods. GFSH exhibits significantly faster dynamics than FSSH. The time scale τ for the Auger process is obtained from the three-parameter exponential fit, $f(x) = a - b\exp(-t/\tau)$. The parameter a represents the initial Gaussian stage of dynamics, which is common to all quantum transitions.[57,62] The 8.2 ps FSSH time is three times longer than 2.8 ps obtained through GFSH. The Auger process is a two-particle reaction, involving simultaneous electron and hole transitions. For example, as shown in Figure 1B, the Auger process starts from the 2 → 4 state and ends in the 1 → 3 state with similar energy. It proceeds via the I−II or III−IV pathways. In either case, transitions into higher energy states are involved, and are classically forbidden in FSSH. In contrast, GFSH can realize the two-particle transfer within one time step. The observed faster relaxation gives strong evidence that GFSH can reproduce the Auger-type dynamics. Further analysis of the FSSH results indicates that the 8.2 ps time describes the sequential process, first involving thermal excitation of the hole, and then an electron transition from $1P_e$ into $1S_e$ with the hole frozen. Including decoherence effects,[57] or eliminating thermally

dx.doi.org/10.1021/ct5003835 | J. Chem. Theory Comput. 2014, 10, 3598−3605

accessible hole states (currently eliminated only up to 0.1 eV), will dramatically slow down the FSSH dynamics, while the GFSH result will be affected weakly.

In experiment, the two-photon photoemission[50] and transient absorption spectroscopy[63,64] measurements have shown a 0.22 ps time constant for the $1P_e$ to $1S_e$ electron relaxation. The GFSH time scale agrees much better with the experiment than FSSH; however, the obtained electron relaxation is still slow. To explain the discrepancy with the experiment, one needs to bear in mind that the actual QDs are much larger than the adopted demonstration here. Larger QD have much higher density of states, which accelerate the Auger dynamics. Calculations on larger QDs are under way and constitute a subject of a separate study.

4. CONCLUDING REMARKS

Similar to FSSH, GFSH provides a general solution to mixed quantum-classical dynamics. As shown in the above demonstrations, GFSH is advantageous to FSSH when encountering classically forbidden transitions, as exemplified by the superexchange mechanism. GFSH does not eliminate classically forbidden transitions, which are essential for achieving the detailed balance. Rather, GFSH allows superexchange that cannot happen in FSSH due to forbidden hops. GFSH possesses several other advantages. In our recent publication,[36] a self-consistency test is proposed to correct the FSSH probabilities during trivial crossings. GFSH automatically fulfills the self-consistency test, because the expression for the surface hopping probabilities does not contain the nonadiabatic coupling constant anymore. One can carry out wave function propagation accurately in a suitable representation (e.g., the "diabatic" atomic orbital basis, a plane-wave basis, or a spatial grid)[65−67] and then compute the population change in the preferred surface hopping basis through a representation transformation. The preferred, often adiabatic, basis can be used to perform GFSH avoiding the trivial crossings problem altogether. Further, GFSH can be combined with the flexible surface hopping (FSH) idea, which can greatly reduce the computational cost for nonadiabatic molecular dynamics in large systems. There, we can use the population change of each state to determine which states should be included in the flexible system for surface hopping. Additional investigations of the GFSH algorithm should involve detailed balance and thermal equilibrium, which are particularly important for studies of relaxation processes in large systems. It would be valuable to incorporate decoherence effects into GFSH.[68−72] Decoherence is needed for proper descriptions of slow transitions between states separated by significant energy gaps. Zero-point energy and quantum mechanical tunneling of nuclei are absent in the current version of GFSH and can be added using semiclassical techniques.[73,74]

In summary, we have proposed a novel GFSH method based on quantum population flow. It has been proven to maintain the internal consistency, and thus to possess the same level of theoretical foundation as the standard FSSH. We have applied GFSH to superexchange models and have found that GFSH generally surpasses FSSH. As a practical demonstration, GFSH has been implemented to study Auger processes in quantum dots. It is found that FSSH greatly underestimates the Auger rate, and the mechanism is qualitatively incorrect. GFSH performs much better, since it does allow simultaneous two-particle Auger-like transitions. GFSH can realize population exchange between indirectly coupled states, and improve strongly the performance when classically forbidden transitions are encountered. The present studies indicate that GFSH can replace FSSH, although further tests and investigations are definitely required.

AUTHOR INFORMATION

Corresponding Authors

*Email: linjun.wang@rochester.edu.

*Email: oleg.prezhdo@rochester.edu.

Notes

The authors declare no competing financial interest.

ACKNOWLEDGMENTS

We thank Dr. Alexey V. Akimov for helpful discussions. This work is supported by the U.S. National Science Foundation, Grant No. CHE-1300118.

REFERENCES

(1) Hammes-Schiffer, S.; Tully, J. C. *J. Chem. Phys.* **1994**, *101*, 4657−4667.
(2) Wu, X.; Thiel, W.; Pezeshki, S.; Lin, H. *J. Chem. Theory Comput.* **2013**, *9*, 2672−2686.
(3) Akimov, A. V.; Prezhdo, O. V. *J. Chem. Theory Comput.* **2013**, *9*, 4959−4972.
(4) Akimov, A. V.; Prezhdo, O. V. *J. Chem. Theory Comput.* **2014**, *10*, 789−804.
(5) Stehr, V.; Fink, R. F.; Engels, B.; Pflaum, J.; Deibel, C. *J. Chem. Theory Comput.* **2014**, *10*, 1242−1255.
(6) Uspenskiy, I.; Strodel, B.; Stock, G. *J. Chem. Theory Comput.* **2006**, *2*, 1605−1617.
(7) Landry, B. R.; Subotnik, J. E. *J. Chem. Phys.* **2011**, *135*, 191101.
(8) Xie, W.; Bai, S.; Zhu, L.; Shi, Q. *J. Phys. Chem. A* **2013**, *117*, 6196−6204.
(9) Wang, L.; Beljonne, D.; Chen, L.; Shi, Q. *J. Chem. Phys.* **2011**, *134*, 244116.
(10) Wang, L.; Beljonne, D. *J. Phys. Chem. Lett.* **2013**, *4*, 1888−1894.
(11) Wang, L.; Beljonne, D. *J. Chem. Phys.* **2013**, *139*, 064316.
(12) Kraack, J. P.; Buckup, T.; Motzkus, M. *J. Phys. Chem. Lett.* **2013**, *4*, 383−387.
(13) Fingerhut, B. P.; Dorfman, K. E.; Mukamel, S. *J. Chem. Theory Comput.* **2014**, *10*, 1172−1188.
(14) Herman, M. F. *Annu. Rev. Phys. Chem.* **1994**, *45*, 83−111.
(15) Kapral, R. *Annu. Rev. Phys. Chem.* **2006**, *57*, 129−157.
(16) Gorshkov, V. N.; Tretiak, S.; Mozyrsky, D. *Nat. Commun.* **2013**, *4*, 2144.
(17) Parandekar, P. V.; Tully, J. C. *J. Chem. Phys.* **2005**, *122*, 094102.
(18) Parandekar, P. V.; Tully, J. C. *J. Chem. Theory Comput.* **2006**, *2*, 229−235.
(19) Ehrenfest, P. *Z. Phys.* **1927**, *45*, 455−457.
(20) Prezhdo, O. V.; Kisil, V. V. *Phys. Rev. A* **1997**, *56*, 162−175.
(21) Tully, J. C. *J. Chem. Phys.* **1990**, *93*, 1061−1071.
(22) Drukker, K. *J. Comput. Phys.* **1999**, *153*, 225−272.
(23) Barbatti, M. *WIREs Comput. Mol. Sci.* **2011**, *1*, 620−633.
(24) Tully, J. C. *J. Chem. Phys.* **2012**, *137*, 22A301.
(25) Tapavicza, E.; Tavernelli, I.; Rothlisberger, U. *Phys. Rev. Lett.* **2007**, *98*, 023001.
(26) Nelson, T.; Fernandez-Alberti, S.; Chernyak, V.; Roitberg, A. E.; Tretiak, S. *J. Phys. Chem. B* **2011**, *115*, 5402−5414.
(27) Tapavicza, E.; Bellchambers, G. D.; Vincent, J. C.; Furche, F. *Phys. Chem. Chem. Phys.* **2013**, *15*, 18336−18348.
(28) Ren, J.; Vukmirović, N.; Wang, L.-W. *Phys. Rev. B* **2013**, *87*, 205117.
(29) Duncan, W. R.; Prezhdo, O. V. *Annu. Rev. Phys. Chem.* **2007**, *58*, 143−184.
(30) Jaeger, H. M.; Kim, H.-D.; Prezhdo, O. V. *Acc. Chem. Res.* **2013**, *46*, 1280−1289.

(31) Akimov, A. V.; Neukirch, A. J.; Prezhdo, O. V. *Chem. Rev.* **2013**, *113*, 4496−4565.
(32) Granucci, G.; Persico, M.; Toniolo, A. *J. Chem. Phys.* **2001**, *114*, 10608−10615.
(33) Fabiano, E.; Keal, T. W.; Thiel, W. *Chem. Phys.* **2008**, *349*, 334−347.
(34) Evenhuis, C.; Martínez, T. J. *J. Chem. Phys.* **2011**, *135*, 224110.
(35) Fernandez-Alberti, S.; Roitberg, A. E.; Nelson, T.; Tretiak, S. *J. Chem. Phys.* **2012**, *137*, 014512.
(36) Wang, L.; Prezhdo, O. V. *J. Phys. Chem. Lett.* **2014**, *5*, 713−719.
(37) Jasper, A. W.; Hack, M. D.; Truhlar, D. G. *J. Chem. Phys.* **2001**, *115*, 1804−1816.
(38) Fang, J.-Y.; Hammes-Schiffer, S. *J. Chem. Phys.* **1999**, *110*, 11166−11175.
(39) Fang, J.-Y.; Hammes-Schiffer, S. *J. Phys. Chem. A* **1999**, *103*, 9399−9407.
(40) Jasper, A. W.; Stechmann, S. N.; Truhlar, D. G. *J. Chem. Phys.* **2002**, *116*, 5424−5431.
(41) Jasper, A. W.; Truhlar, D. G. *Chem. Phys. Lett.* **2003**, *369*, 60−67.
(42) Granucci, G.; Persico, M. *J. Chem. Phys.* **2007**, *126*, 134114.
(43) Smith, M. B.; Michl, J. *Chem. Rev.* **2010**, *110*, 6891−6936.
(44) Berkelbach, T. C.; Hybertsen, M. S.; Reichman, D. R. *J. Chem. Phys.* **2013**, *138*, 114102.
(45) Beljonne, D.; Yamagata, H.; Brédas, J. L.; Spano, F. C.; Olivier, Y. *Phys. Rev. Lett.* **2013**, *110*, 226402.
(46) Akimov, A. V.; Prezhdo, O. V. *J. Am. Chem. Soc.* **2014**, *136*, 1599−1608.
(47) Lee, J.; Jadhav, P.; Reusswig, P. D.; Yost, S. R.; Thompson, N. J.; Congreve, D. N.; Hontz, E.; Van Voorhis, T.; Baldo, M. A. *Acc. Chem. Res.* **2013**, *46*, 1300−1311.
(48) Seidel, W.; Titkov, A.; André, J. P.; Voisin, P.; Voos, M. *Phys. Rev. Lett.* **1994**, *73*, 2356−2359.
(49) Hartmann, T.; Reineker, P.; Yudson, V. I. *Phys. Rev. B* **2011**, *84*, 245317.
(50) Sippel, P.; Albrecht, W.; Mitoraj, D.; Eichberger, R.; Hannappel, T.; Vanmaekelbergh, D. *Nano Lett.* **2013**, *13*, 1655−1661.
(51) Kosloff, D.; Kosloff, R. *J. Comput. Phys.* **1983**, *52*, 35−53.
(52) Van Loan, C. *Computational Frameworks for the Fast Fourier Transform*; Society for Industrial and Applied Mathematics: Philadelphia, 1992.
(53) Press, W. H.; Teukolsky, S. A.; Vetterling, W. T.; Flannery, B. P. *Numerical Recipes*; Cambridge University Press: Cambridge, U.K., 1992.
(54) Subotnik, J. E. *J. Phys. Chem. A* **2011**, *115*, 12083−12096.
(55) Ross, R. T.; Nozik, A. J. *J. Appl. Phys.* **1982**, *53*, 3813−3818.
(56) Nozik, A. J. *Annu. Rev. Phys. Chem.* **2001**, *52*, 193−231.
(57) Kilina, S. V.; Neukirch, A. J.; Habenicht, B. F.; Kilin, D. S.; Prezhdo, O. V. *Phys. Rev. Lett.* **2013**, *110*, 180404.
(58) Kresse, G.; Hafner, J. *Phys. Rev. B* **1993**, *47*, 558−561.
(59) Kresse, G.; Hafner, J. *Phys. Rev. B* **1994**, *49*, 14251−14269.
(60) Kresse, G.; Furthmüller, J. *Phys. Rev. B* **1996**, *54*, 11169−11186.
(61) Prezhdo, O. V.; Duncan, W. R.; Prezhdo, V. V. *Prog. Surf. Sci.* **2009**, *84*, 30−68.
(62) Long, R.; English, N. J.; Prezhdo, O. V. *J. Am. Chem. Soc.* **2013**, *135*, 18892−18900.
(63) Klimov, V. I.; McBranch, D. W. *Phys. Rev. Lett.* **1998**, *80*, 4028−4031.
(64) Klimov, V. I.; McBranch, D. W.; Leatherdale, C. A.; Bawendi, M. G. *Phys. Rev. B* **1999**, *60*, 13740−13749.
(65) Yabana, K.; Bertsch, G. F. *Phys. Rev. B* **1996**, *54*, 4484−4487.
(66) Burdick, W. R.; Saad, Y.; Kronik, L.; Vasiliev, I.; Jain, M.; Chelikowsky, J. R. *Comput. Phys. Commun.* **2003**, *156*, 22−42.
(67) Andrade, X.; Alberdi-Rodriguez, J.; Strubbe, D. A.; Oliveira, M. J. T.; Nogueira, F.; Castro, A.; Muguerza, J.; Arruabarrena, A.; Louie, S. G.; Aspuru-Guzik, A.; Rubio, A.; Marques, M. A. L. *J. Phys.: Condens. Matter* **2012**, *24*, 233202.
(68) Bittner, E. R.; Rossky, P. J. *J. Chem. Phys.* **1995**, *103*, 8130−8143.
(69) Prezhdo, O. V. *J. Chem. Phys.* **1999**, *111*, 8366−8377.
(70) Hack, M. D.; Truhlar, D. G. *J. Chem. Phys.* **2001**, *114*, 9305−9314.
(71) Bedard-Hearn, M. J.; Larsen, R. E.; Schwartz, B. J. *J. Chem. Phys.* **2005**, *123*, 234106.
(72) Jaeger, H. M.; Fischer, S.; Prezhdo, O. V. *J. Chem. Phys.* **2012**, *137*, 22A545.
(73) Wang, L.; Akimov, A. V.; Chen, L.; Prezhdo, O. V. *J. Chem. Phys.* **2013**, *139*, 174109.
(74) Zamstein, N.; Tannor, D. J. *J. Chem. Phys.* **2012**, *137*, 22A517.